Investigations on Grid-Connected DFIWGs Development and Performance Analysis with the Support of Crowbar and STATCOM

Mohamed Metwally Mahmoud [1,*], Idriss Benlaloui [2], Basma Benbouya [3], Nagwa F. Ibrahim [4]
[1] Electrical Engineering Department, Faculty of Energy Engineering, Aswan University, Aswan 81528, Egypt
[2] LSPIE Laboratory, University of Batna 2, Mostefa Ben Boulaid, avenue Med Elhadi, Boukhlouf, Algeria
[3] LSELM, Laboratoire des systemes electromecaniques, Department of Electromechanic, Faculty of Technology, Badji Mokhtar Annaba University, Algeria
[4] Electrical Department, Faculty of Technology and Education, Suez University, Suez 43533, Egypt
Email: [1] metwally_m@aswu.edu.eg, [2] i.benlaloui@univ-batna2.dz, [3] basma.benbouya@univ-annaba.dz, [4] nagwa.ibrahim@ind.suezuni.edu.eg
*Corresponding Author

***Abstract*—These days, one of the most used layouts in the wind power industry is a variable-speed doubly-fed induction wind generator (DFIWG). To provide real and reactive power (P&Q) control during grid failures, this research examines the DFIWG. The system's transient behavior is examined under normal and abnormal conditions. Through rotor side converter (RSC) and grid side converter (GSC) control, Q assistance for the grid, and power converter stress reduction, the suggested control approach achieves system stability while enabling DFIWG to operate smoothly during grid failures. By suppressing rotor and stator overcurrent, DC link voltage (V_{DC}) overshoot, and P&Q oscillations, as well as supporting the grid voltage (GV) under both balanced and unbalanced grid fault scenarios with distinct voltage dips, the suggested technique preserves the system characteristics during grid faults. MATLAB/SIMULINK 2017b is used for time-domain computer simulations. STATCOM and crowbar, two suggested systems, are contrasted. This work proves the effectiveness of the suggested approaches in augmenting the system's fault ride-through (FRT) capacity.**

***Keywords*—Crowbar, Control System, DFIG, STATCOM, Grid Faults**

I. INTRODUCTION

DFIWGs have been exposed to grid disruptions when they were directly connected, via lengthy transmission lines (TLs), to the grid at near-to-ground voltages. In grids, imbalanced GVs are the most prevalent. Unequal GV drops on TLs or unbalanced loads connected at the point of common connection (POCC) can cause imbalanced GV [1]-[4]. As a result, key grid codes were distributed by energy system operators, mandating that DFIWGs be able to sustain a 2% steady-state and 4% short-term imbalance in GV without triggering [5]-[8]. Negative sequence stator/rotor current parts are produced by an imbalanced GV. There will be strong fluctuations in V_{DC}, electromagnetic torque, and power at twofold supply frequency. Consequently, an imbalanced generator voltage can damage generator bearings, V_{DC} at capacitors, and DC/AC inverters. To solve these issues with no disconnecting the generating systems, the DFIWG controller systems must handle these conditions [9]-[12]. GSCs are controlled to regulate V_{DC} and total Q injected into the grid, while RSCs are managed to adjust stator P&Q power [13].

Various control systems, such as vector control (VC) and direct power control (DPC), are investigated to regulate DFIWG in a typical setting [14]-[16]. One of the favored control strategies was the DPC of DFIWG. When weighed against VC, DPC offers some benefits, including ease and quick response time [17], [18]. Under uneven and deformed GV, the functioning of DPC is investigated [19]-[21].

RSC-based DPC was controlled by PI resonant controllers (PIRs) in [22]. To accomplish various control objectives, a power adjustment method (PAM) is included. To obtain the (+ and - sequence) parts of GV and current, nevertheless the stator deconstruction method is necessary. A static target framework DPC-based sliding mode (SM) regulator with a PAM was developed in [23]. A vector-PI (VPI) controller was developed in [24] to enhance the DPC of DFIWG in the presence of harmonic GV. Synchronous relative frame implementation was used for the regulator. DPC and a separated framework for DFIWG that utilizes lagging control are coupled in [19]. Tests are conducted on the suggested controller's functionality in both symmetric voltage dip and typical circumstances. Rather than employing traditional immediate power elements, the DPC method is constructed in [25] utilizing expanded concepts of power. A second-order (SO) generalized integrator (GI) is used to estimate the delayed values and filtered stator voltage. DPC employs frequency adaptive vector PI (FAVPI) in [26] to lessen the impact of harmoniously and imbalanced GV. DAVPI requires an axis conversion and a frequency estimation. A voltage-modulating DPC (VM-DPC) was proposed in [27] to enhance both intermittent and constant-state performance in balance GV scenarios. An additional parallel adjuster is intended to work in tandem with the VM-DPC to regulate (-sequence) current and enhance stator current, active power (P), and reactive power (Q). Nonetheless, the gathering of the voltage and current elements of a stator in (+ and - sequence) is necessary. Ref. [28] uses extended P to build an SM-DPC approach for DFIWG.

In [29], the MP-DPC of RSC under unbalanced GV is examined. Moreover, observations of the rotor current (RC) were necessary for the computation of the rotor voltage (RV) vector. A unified PAM is suggested for a low complexity MP-DPC that was designed in [30], [31]. MP-based RC control for matrix converters was designed in [22]. RV vectors were delivered in [23] during a predetermined sample interval. On the other hand, there might be a rise in shift frequency and losses.

PI regulators (PIR) have been made to function well both in abrupt and stable conditions when it comes to electrical control. Nonetheless, there are two grid frequency (GF) fluctuation elements when the grid is out of sync. Because of the inadequate gain at two times GF, PIR would not be suitable [22]. To address the shortcomings of PIR, PIR was proposed [32]. PIR has the potential to achieve zero steady-state error; however, the pole distribution of the control object DFIWG may cause an unanticipated peak in magnitude response at a GF greater than the resonant frequency, which is harmful to stable closed-loop (CL) operation [33], [34]. Precise AC pulse monitoring and sufficient CL phase tolerance are features of the PIR. PIR can be built to eliminate the DFIWG stator P and Q pulsation components based on pole-zero cancellation to prevent the surprise gain spike [33].

The performance study of DFIWG to the weak grid is examined in this research. To prevent the axial transformation of stator voltage and current, control of the RSC is built on a stationary reference frame. Equations for electromagnetic torque and stator power are derived using rotor flux under balance and imbalanced GV as inputs. To assess the DFIWG's performance, it is used with a crowbar, a FACTS device, and no additional tools. Simulation studies are conducted to assess DFIWG's performance. The performance of several approaches is assessed under balanced and unbalanced GV.

II. Description and Mathematical Modeling of the Investigated System

A. System Description

A two-level IGBT voltage source converter (VSC) system in a back-to-back converter (BTBC) configuration is normally used for DFIWG. Since both stator and rotor can feed energy to the grid, the generator is known as DFIWG. For grid-connected DFIWG, the stator is directly connected to the grid, and the rotor is connected to the grid through BTBC. The power converter of the rotor consists of two components, the RSC and GSC, which are controlled independently [35]-[38].

RSC is used to provide the required magnetizing current in the rotor winding for controlling P and Q which flow from the stator terminals of DFIWG to the grid. The main task of the GSC is to keep the DCLV constant. This system allows a variable speed operation over a range of (+/ -) 30% around the synchronous speed. Therefore, the power flow in the rotor circuit is bidirectional: it can flow from the grid to the rotor or vice versa. This requires a four-quadrant converter system as shown in Fig. 1. However, the converter system needs to process only around 30% of the rated power. The use of reduced-capacity converters results in a reduction in cost, weight, and physical size as well [39]-[41].

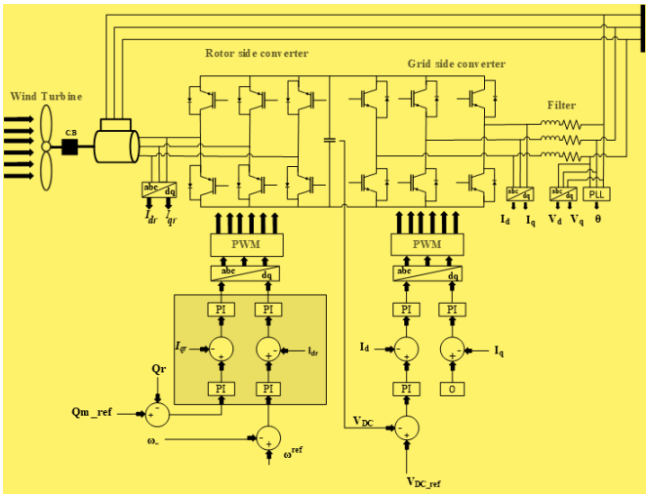

Fig. 1. Grid-tied DFIWG

B. Mathematical Model

A mathematical model of DFIWG, derived in an appropriate dq frame reference is established. The grid voltage-oriented VC is used for GSC to maintain a constant DCLV and to compensate for Q at the network. The stator field-oriented VC is adopted in the RSC control strategy, providing efficient handling of P and Q at the stator [40], [42]. The winding arrangement of the asymmetrical induction machine (IM) is shown in Fig. 2 [43], [44].

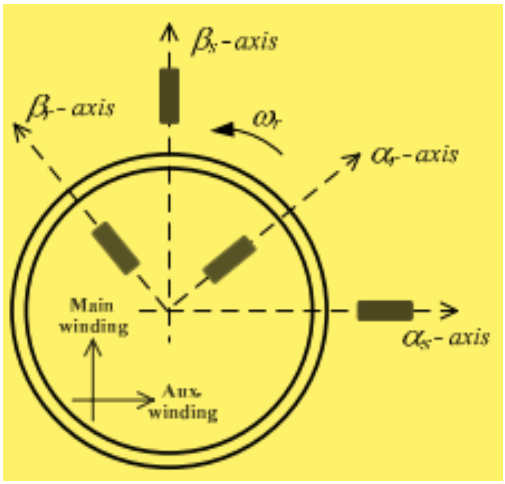

Fig. 2. Configuration of the winding for IMs

The equivalent circuit diagram of an IM is shown in Fig. 3 and Fig. 4. In these Figs, the IM is represented as a two-phase machines. For the modeling of DFIWG in a synchronously rotating frame reference, we need to represent the two-phase stator (ds-qs) and rotor (dr-qr) circuit variables in a synchronously rotating (d-q) frame [45], [46].

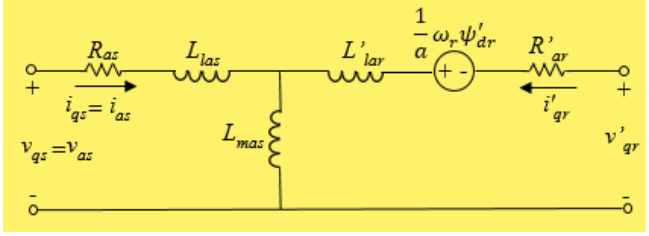

Fig. 3. Dynamic d-q equivalent circuit of DFIG (q-axis circuit)

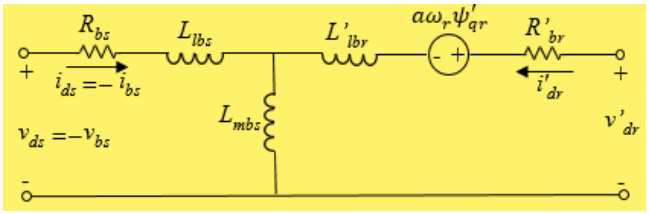

Fig. 4. Dynamic d-q equivalent circuit of DFIG (d-axis circuit)

The stator circuit equations are represented by equations (1) and (2), and rotor circuit equations are represented by equations (3) and (4) given:

$$V_{ds} = R_S\, I_{ds} - \frac{d\psi_{ds}}{dt} - \omega_S\, \psi_{qs} \tag{1}$$

$$V_{qs} = R_S\, I_{qs} + \frac{d\psi_{qs}}{dt} + \omega_S\, \psi_{ds} \tag{2}$$

$$V_{dr} = R_r\, I_{dr} + \frac{d\psi_{dr}}{dt} - (\omega_S - \omega_r)\, \psi_{qr} \tag{3}$$

$$V_{qr} = R_r\, I_{qr} + \frac{d\psi_{qr}}{dt} + (\omega_S - \omega_r)\, \psi_{dr} \tag{4}$$

$$\psi_{ds} = L_s\, I_{ds} + L_m\, I_{dr} \tag{5}$$

$$\psi_{qs} = L_s\, I_{qs} + L_m\, I_{qs} \tag{6}$$

$$\psi_{dr} = L_r\, I_{dr} + L_m\, I_{dr} \tag{7}$$

$$\psi_{qr} = L_r\, I_{qr} + L_m\, I_{qs} \tag{8}$$

$$T_e = \frac{3}{2}\, P\, (\psi_{ds}\, I_{qs} - \psi_{qs}\, I_{ds}) \tag{9}$$

Where all the variables are in a synchronously rotating frame. The bracketed terms are defined as the back e.m.f. or counter e.m.f due to the rotation of axes as in the case of DC machines. When the angular speed ω_r = zero the speed e.m.f due to the d and q axis is zero and the equations change to the stationary form.

Owing to the rotor circuit, if the rotor is blocked or not moving, i.e. ω_r=0, the machine equations can be written similarly to stator equations as in 3 and 4. All the parameters are referred to the primary circuit, which is a stator in this case. Let the rotor rotate at an ω_r, then the d-q axes fixed on the rotor fictitiously will move at a relative speed ω_S-ω_r. The flux linkage expressions in terms of current can be written from Fig. 3 and Fig. 4 as in (5)-(8).

Equation (1) to equation (8) describes the complete electrical modeling of DFIWG. Whereas Eq. (9) expresses the relations of mechanical parameters which are an essential part of the modeling.

C. Control Of DFIWG

Fig. 5 shows the block diagram of DFIWG with stator voltage-oriented control (SVOC). The abc /dq and dq/abc transformation blocks transform the variables in the abc stationary reference frame to the dq synchronous reference frame, and vice versa. The angle of the SVOC can be obtained via the measured 3-phase stator voltages [47], [48].

The MPPT block generates the reference torque based on the optimal torque method. The reference for the d-axis rotor current is calculated according to equation (3). For a given stator Qs*, the q-axis rotor current reference is calculated by equation (4). The reference dq-axis currents are then compared to the measured values, and the errors are passed through PI controllers. The output of the PI controllers is the dq-axis rotor voltage references in the synchronous frame, which are transformed into a three-phase reference for rotor voltages in the stationary frame. The rotor reference voltages can serve as the three-phase modulating waveforms in carrier-based modulation schemes or be converted into a reference space vector for the space vector modulation (SVM). PWM block generates gating signals for the RSC. The GSC performs two main functions: (1) it keeps the V_{DC} constant, and (2) provides Q to the grid when required. The Q reference can be set to zero for the unity power factor (UPF) operation of the converter. The overall PF of the DFIWG is then controlled by the RSC [49]-[52].

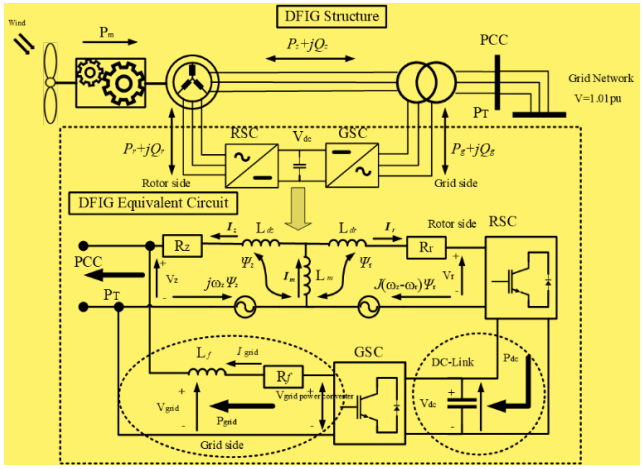

Fig. 5. Block diagram of a DFIG with stator voltage-oriented control

III. Simulation Results and Discussion

Simulation has been done on a 1.5 MW, 575V, 50 Hz, 3 poles DFIWG by using MATLAB/Simulink [10]. Studying DFIWG performance includes time response of P, Q, and V_{DC} during normal and abnormal conditions. Active crowbar (AC) and STATCOM devices are used for enhancement of their performance, and their connections are illustrated in Fig. 6. The investigated configurations show the role of these suggested tools. In the obtained results, C1, C2, and C3 represent without protection, with STATCOM, and with AC, respectively.

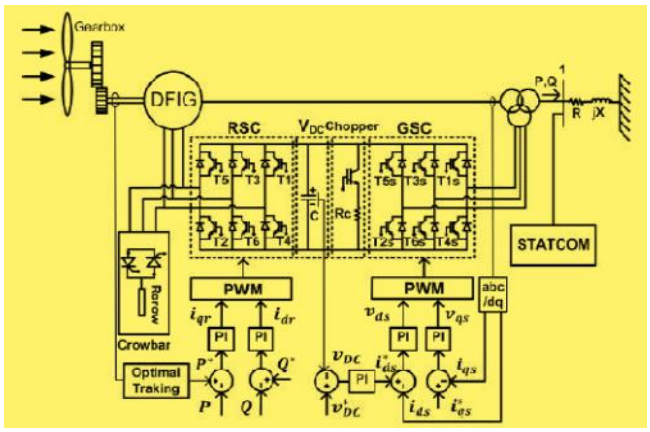

Fig. 6. Schematic diagram of AC and STATCOM with DFIWG

A. *Studying the Performance of DFIG Under Starting*

Fig. 7 from (a) to (c) shows the performance of grid-connected DFIWG in the case of balanced grid operation. Set point P=1.5 MW and Q=0 which means that DFIWG is operated at unity power factor. The V_{DC} is maintained constant at 1150 V. Results show that both STATCOM and AC enhanced the dynamic performance of DFIWG as shown in Fig. 7.

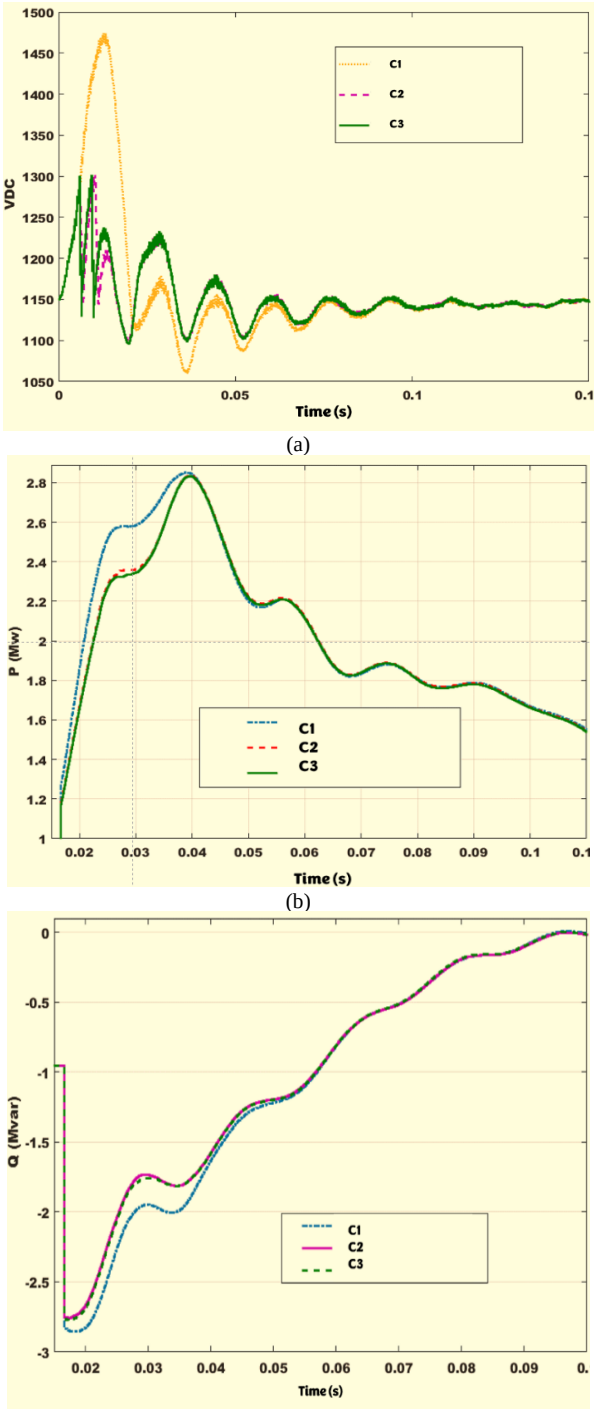

(a)

(b)

(c)

Fig. 7. Simulation results (a) V_{DC}, (b) P, (c) Q

B. *Studying The Dynamic Performance of DFIG Under Three Phases to Ground Fault*

Dynamic performance of the system is studied AC and STATCOM. This fault leads to the voltage decreasing to zero roughly. In this paper assumption of GV disturbance occurs at t=0.25 s and cleared at 0.3 s. During the fault period, the P decreased to zero, and after fault clearing P returned to its rated value of 1.5 MW as seen in Fig. 8 (b), but Q drawn from the grid increased during the fault period which reached 1 Mvar roughly and after fault clearing Q returns to its rated value 0 as seen in Fig. 8 (c). The V_{DC} increased during the fault period to reach 1800 V, but AC and STATCOM decreased to reach 1300 V which protects the back-to-back converter from damage as seen in Fig. 8 (a). Fig. 9 (a-c) shows STATCOM has a superior performance compared to AC and without protection. DFIWG is still connected to the grid and Q supply is found to mean FRT capability realization.

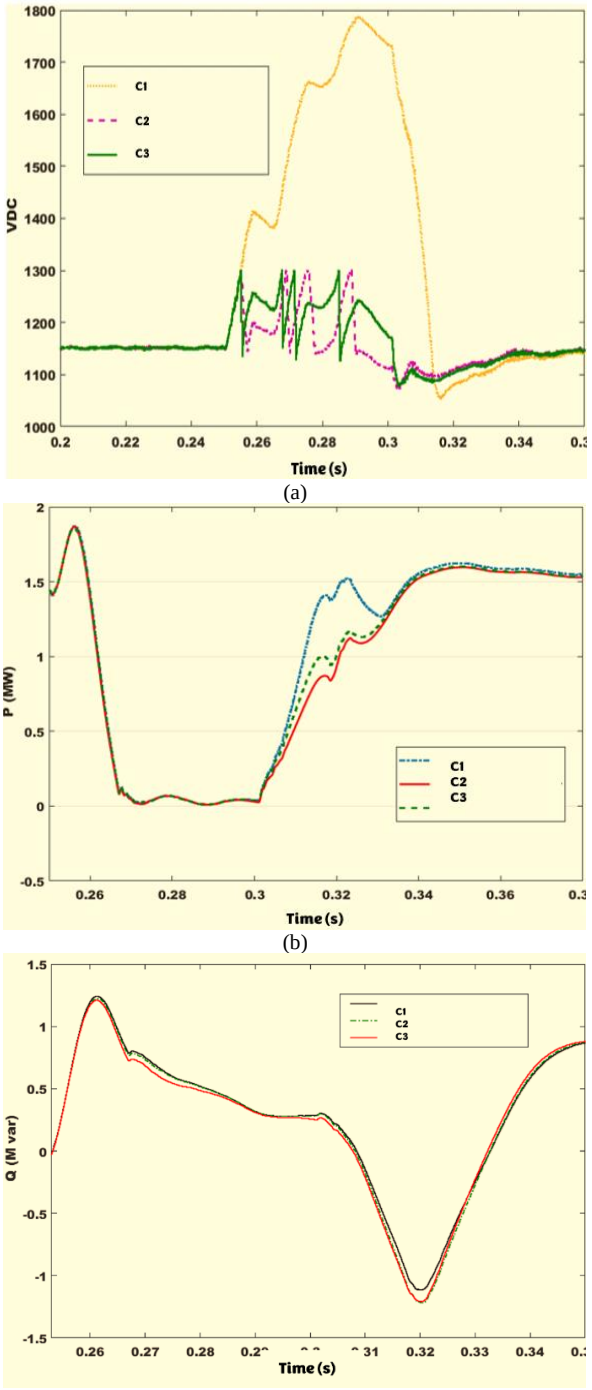

(a)

(b)

(c)

Fig. 8. Simulation results (a) V_{DC}, (b) P, (c) Q

C. *Studying the Dynamic Performance of DFIG Under Double Line to Ground Fault*

At the occurrence of this fault, the P drops to nearly 0.5 MW with AC and reaches 0.62 MW with STATCOM as shown in Fig. 9 (b). The V_{DC} reaches about 1330 V without protection and reaches 1250 V with STATCOM but with AC reaches 1200 V only as seen in Fig. 9 (a). The DFIWG absorbs about 1 Mvar during the fault period but STATCOM gives better performance for P&Q during the fault period compared to AC as depicted in Fig. 9 (c). Although AC gives better performance for the V_{DC}.

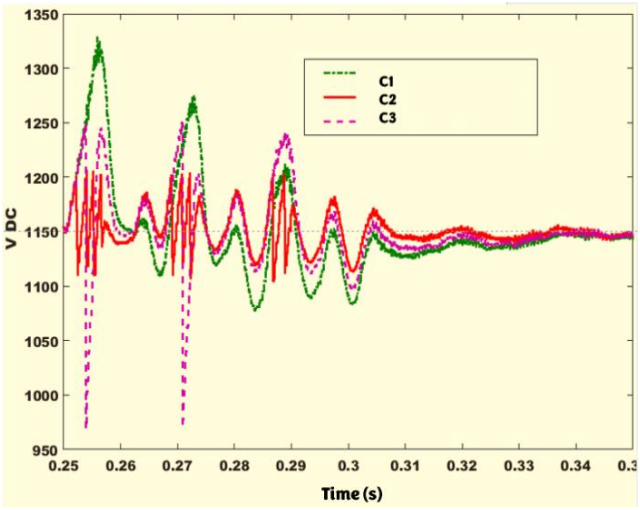

(a)

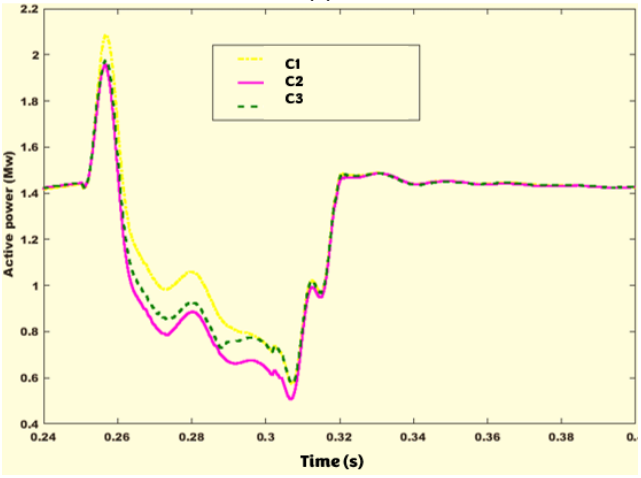

(b)

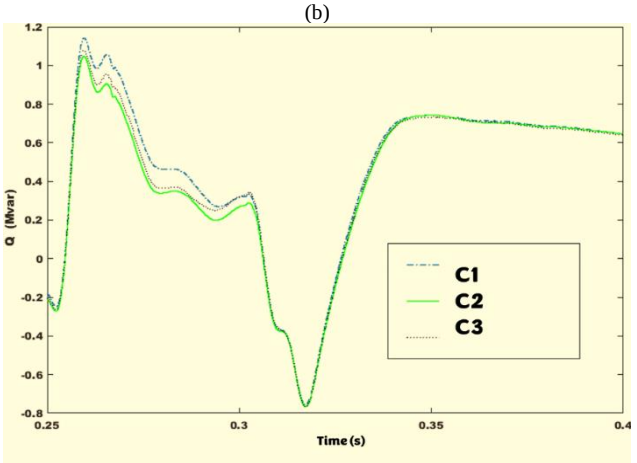

(c)

Fig. 9. Simulation results (a) VDC, (b) P, (c) Q

IV. CONCLUSION

When failures occur, DFIWG is under a lot of stress. By using an AC and STATCOM, DFIWG may remain connected to the grid and restrict currents and voltages below predetermined thresholds. The Q regulation cannot be provided by DFIWG equipped with AC, although it can withstand grid disturbances, according to simulations. Investigations are conducted into the use of a STATCOM linked to a DFIWG to enable uninterruptible FRT of GV faults. Whereas the DFIWG can carry on with its nominal operation and satisfy any grid code requirement without requiring additional protective mechanisms, the STATCOM can make up for the defective line voltage. Simulation results declared that the dip in GV leads to overvoltage in the DC link and a decrease in P. From the previous discussion, we find that the DFIWG connected to the grid gives a better dynamic performance with the STATCOM tool in case of three-phase fault and double line to ground fault compared to AC. AC and STATCOM tools have succeeded in enhancing the machine's performance.

REFERENCES

[1] P. Cheng and H. Nian, "Collaborative Control of DFIG System During Network Unbalance Using Reduced-Order Generalized Integrators," *IEEE Transactions on Energy Conversion*, vol. 30, no. 2, pp. 453-464, 2015, https://doi.org/10.1109/TEC.2014.2363671.

[2] D. Yang *et al*., "Sequential frequency regulation strategy for DFIG and battery energy storage system considering artificial deadbands," *International Journal of Electrical Power & Energy Systems*, vol. 155, p. 109503, 2024, https://doi.org/10.1016/j.ijepes.2023.109503.

[3] M. M. Mahmoud, "Improved current control loops in wind side converter with the support of wild horse optimizer for enhancing the dynamic performance of PMSG-based wind generation system," *International Journal of Modelling and Simulation*, vol. 43, no. 6, pp. 952–966, 2023, https://doi.org/10.1080/02286203.2022.2139128.

[4] M. M. Mahmoud, M. Khalid Ratib, M. M. Aly, and A. M. M. Abdel-Rahim, "Wind-driven permanent magnet synchronous generators connected to a power grid: Existing perspective and future aspects," *Wind Engineering*, vol. 46, no. 1, pp. 189–199, 2022, https://doi.org/10.1177/0309524X211022728.

[5] Z. Hao, Z. Fuhong, G. Ziming, G. Zeping, "Study on regulation and control of active wind power fluctuations," *Information Technology Journal*, vol. 13, no. 18, pp. 2743-2748, 2014, https://doi.org/10.3923/itj.2014.2743.2748.

[6] M. M. Mahmoud *et al*., "Evaluation and Comparison of Different Methods for Improving Fault Ride-Through Capability in Grid-Tied Permanent Magnet Synchronous Wind Generators," *International Transactions on Electrical Energy Systems*, vol. 2023, no. 1, pp. 1-22, 2023, https://doi.org/10.1155/2023/7717070.

[7] M. Awad *et al*., "A review of water electrolysis for green hydrogen generation considering PV/wind/hybrid/hydropower/geothermal/tidal and wave/biogas energy systems, economic analysis, and its application," *Alexandria Engineering Journal*, vol. 87, pp. 213–239, 2024, https://doi.org/10.1016/j.aej.2023.12.032.

[8] A. T. Hassan *et al*., "Adaptive Load Frequency Control in Microgrids Considering PV Sources and EVs Impacts: Applications of Hybrid Sine Cosine Optimizer and Balloon Effect Identifier Algorithms," *International Journal of Robotics and Control Systems*, vol. 4, no. 2, pp. 941-957, 2024, https://doi.org/10.31763/ijrcs.v4i2.1448.

[9] Y. Moumani, A. J. Laafou, and A. A. Madi, "A comparative study based on proportional integral and backstepping controllers for doubly fed induction generator used in wind energy conversion system," *Archives of Electrical Engineering*, vol. 72, no. 1, pp. 211-228, 2023, https://doi.org/10.24425/aee.2023.143698.

[10] M. M. Mahmoud, B. S. Atia, A. Y. Abdelaziz, and N. A. N. Aldin, "Dynamic Performance Assessment of PMSG and DFIG-Based WECS with the Support of Manta Ray Foraging Optimizer Considering MPPT, Pitch Control, and FRT Capability Issues," *Processes*, vol. 10,

no. 12, p. 2723, 2022, https://doi.org/10.3390/pr10122723.

[11] M. M. Mahmoud *et al.*, "Application of Whale Optimization Algorithm Based FOPI Controllers for STATCOM and UPQC to Mitigate Harmonics and Voltage Instability in Modern Distribution Power Grids," *Axioms*, vol. 12, no. 5, p. 420, 2023, https://doi.org/10.3390/axioms12050420.

[12] N. F. Ibrahim *et al*., "Operation of Grid-Connected PV System With ANN-Based MPPT and an Optimized LCL Filter Using GRG Algorithm for Enhanced Power Quality," *IEEE Access*, vol. 11, pp. 106859-106876, 2023, https://doi.org/10.1109/ACCESS.2023.3317980.

[13] H. Alnami, "Study of the Crowbar's Functioning in Doubly Fed Induction Wind Generators: Towards Achieving Fault Ride Through Capability," *International Journal of Robotics and Control Systems*, vol. 4, no. 3, pp. 1304-1318, 2024, https://doi.org/10.31763/ijrcs.v4i3.1485.

[14] E. Tremblay, S. Atayde and A. Chandra, "Comparative Study of Control Strategies for the Doubly Fed Induction Generator in Wind Energy Conversion Systems: A DSP-Based Implementation Approach," *IEEE Transactions on Sustainable Energy*, vol. 2, no. 3, pp. 288-299, 2011, https://doi.org/10.1109/TSTE.2011.2113381.

[15] I. E. Maysse *et al*., "Nonlinear Observer-Based Controller Design for VSC-Based HVDC Transmission Systems Under Uncertainties," *IEEE Access*, vol. 11, pp. 124014-124030, 2023, https://doi.org/10.1109/ACCESS.2023.3330440.

[16] I. E. Maysse *et al*., "Nonlinear Observer-Based Controller Design for VSC-Based HVDC Transmission Systems Under Uncertainties," *IEEE Access*, vol. 11, pp. 124014-124030, 2023, https://doi.org/10.1109/ACCESS.2023.3330440.

[17] H. A. Aroussi, E. M. Ziani, M. Bouderbala, and B. Bossoufi, "Enhancement of the direct power control applied to DFIG-WECS," *International Journal of Electrical and Computer Engineering*, vol. 10, no. 1, pp. 35-46, 2020, http://doi.org/10.11591/ijece.v10i1.pp35-46.

[18] F. Menzri, T. Boutabba, I. Benlaloui, H. Bawayan, M. I. Mosaad, and M. M. Mahmoud, "Applications of hybrid SMC and FLC for augmentation of MPPT method in a wind-PV-battery configuration," *Wind Engineering*, 2024, https://doi.org/10.1177/0309524X241254364.

[19] J. S. Solís-Chaves, M. S. Barreto, M. B. C. Salles, V. M. Lira, R. V. Jacomini, and A. J. S. Filho, "A direct power control for DFIG under a three phase symmetrical voltage sag condition," *Control Engineering Practice*, vol. 65, pp. 48-58, 2017, https://doi.org/10.1016/j.conengprac.2017.05.002.

[20] A. H. Elmetwaly *et al*., "Modeling, Simulation, and Experimental Validation of a Novel MPPT for Hybrid Renewable Sources Integrated with UPQC: An Application of Jellyfish Search Optimizer," *Sustainability*, vol. 15, no. 6, p. 5209, 2023, https://doi.org/10.3390/su15065209.

[21] M. M. Mahmoud, M. K. Ratib, M. M. Aly, and A. M. M. Abdel–Rahim, "Application of Whale Optimization Technique for Evaluating the Performance of Wind-Driven PMSG Under Harsh Operating Events," *Process Integration and Optimization for Sustainability*, vol. 6, pp. 447-470, 2022, https://doi.org/10.1007/s41660-022-00224-8.

[22] E. G. Shehata, "Active and reactive power control of doubly fed induction generators for wind energy generation under unbalanced grid voltage conditions," *Electric Power Components and Systems*, vol. 41, no. 6, pp. 619-640, 2013, https://doi.org/10.1080/15325008.2013.763308.

[23] K. Roummani *et al*., "A new concept in direct-driven vertical axis wind energy conversion system under real wind speed with robust stator power control," *Renewable Energy*, vol. 143, pp. 478-487, 2019, https://doi.org/10.1016/j.renene.2019.04.156.

[24] F. Valenciaga, R. D. Fernández, and F. Inthamoussou, "A second order sliding power control & resonant filtering approach to mitigate grid unbalance effects on a DOIG wind energy based system," *International Conference on Renewable Energies and Power Quality*, vol. 1, no. 15, pp. 255-260, 2017, https://doi.org/10.24084/repqj15.286.

[25] Y. Zhang, J. Jiao and D. Xu, "Direct Power Control of Doubly Fed Induction Generator Using Extended Power Theory Under Unbalanced Network," *IEEE Transactions on Power Electronics*, vol. 34, no. 12, pp. 12024-12037, 2019, https://doi.org/10.1109/TPEL.2019.2906013.

[26] S. Tohidi and M. I. Behnam, "A comprehensive review of low voltage ride through of doubly fed induction wind generators," *Renewable and Sustainable Energy Reviews*, vol. 57, p. 412-419, 2016, https://doi.org/10.1016/j.rser.2015.12.155.

[27] S. Gao, H. Zhao, Y. Gui, D. Zhou, V. Terzija and F. Blaabjerg, "A Novel Direct Power Control for DFIG With Parallel Compensator Under Unbalanced Grid Condition," *IEEE Transactions on Industrial Electronics*, vol. 68, no. 10, pp. 9607-9618, 2021, https://doi.org/10.1109/TIE.2020.3022495.

[28] H. Benbouhenni, F. Mehedi, and L. Soufiane, "New direct power synergetic-SMC technique based PWM for DFIG integrated to a variable speed dual-rotor wind power," *Automatika*, vol. 63, no. 4, pp. 718-731, 2022, https://doi.org/10.1080/00051144.2022.2065801.

[29] Y. Zhang, J. Jiao, D. Xu, D. Jiang, Z. Wang and C. Tong, "Model Predictive Direct Power Control of Doubly Fed Induction Generators Under Balanced and Unbalanced Network Conditions," *IEEE Transactions on Industry Applications*, vol. 56, no. 1, pp. 771-786, 2020, https://doi.org/10.1109/TIA.2019.2947396.

[30] C. Cheng, P. Cheng, H. Nian, and D. Sun, "Model predictive stator current control of doubly fed induction generator during network unbalance," *IET Power Electronics*, vol. 11, no. 1, pp. 120-128, 2018, https://doi.org/10.1049/iet-pel.2017.0049.

[31] X. Ran, B. Xu, K. Liu and J. Zhang, "An Improved Low-Complexity Model Predictive Direct Power Control With Reduced Power Ripples Under Unbalanced Grid Conditions," *IEEE Transactions on Power Electronics*, vol. 37, no. 5, pp. 5224-5234, 2022, https://doi.org/10.1109/TPEL.2021.3131794.

[32] H. Chojaa *et al*., "Nonlinear Control Strategies for Enhancing the Performance of DFIG-Based WECS under a Real Wind Profile," *Energies*, vol. 15, no. 18, p. 6650, 2022, https://doi.org/10.3390/en15186650.

[33] M. Wu, L. Ding, C. Xue and Y. W. Li, "Model-Based Closed-Loop Control for High-Power Current Source Rectifiers Under Selective Harmonic Elimination/Compensation PWM With Fast Dynamics," in *IEEE Journal of Emerging and Selected Topics in Power Electronics*, vol. 10, no. 5, pp. 5921-5932, 2022, https://doi.org/10.1109/JESTPE.2022.3152494.

[34] C. Liu, W. Chen, F. Blaabjerg and D. Xu, "Optimized design of resonant controller for stator current harmonic compensation in DFIG wind turbine systems," *2012 Twenty-Seventh Annual IEEE Applied Power Electronics Conference and Exposition (APEC)*, pp. 2038-2044, 2012, https://doi.org/10.1109/APEC.2012.6166102.

[35] Z. Zheng, G. Yang, and H. Geng, "Coordinated control of a doubly-fed induction generator-based wind farm and a static synchronous compensator for low voltage ride-through grid code compliance during asymmetrical grid faults," *Energies*, vol. 6, no. 9, pp. 4660-4681, 2013, https://doi.org/10.3390/en6094660.

[36] N. F. Ibrahim *et al*., "Multiport Converter Utility Interface with a High-Frequency Link for Interfacing Clean Energy Sources (PV\Wind\Fuel Cell) and Battery to the Power System: Application of the HHA Algorithm," *Sustainability*, vol. 15, no. 18, p. 13716, 2023, https://doi.org/10.3390/su151813716.

[37] H. Boudjemai *et al*., "Experimental Analysis of a New Low Power Wind Turbine Emulator Using a DC Machine and Advanced Method for Maximum Wind Power Capture," *IEEE Access*, vol. 11, pp. 92225-92241, 2023, https://doi.org/10.1109/ACCESS.2023.3308040.

[38] M. F. Elnaggar, "Design and Implementation of Crowbar and STATCOM for Enhanced Stability of Grid-Tied Doubly Fed Induction Wind Generators," *International Journal of Robotics and Control Systems*, vol. 4, no. 3, pp. 1263-1278, 2024, https://doi.org/10.31763/ijrcs.v4i3.1498.

[39] M. E. B. Aguilar, D. V. Coury, R. Reginatto, R. M. Monaro, P. T. de Godoy, and T. G. Jahn, "Multi-Objective PSO for Control-Loop Tuning of DFIG Wind Turbines with Chopper Protection and Reactive-Current Injection," *Energies*, vol. 17, no. 1, p. 28, 2024, https://doi.org/10.3390/en17010028.

[40] A. A. Chhipą *et al*., "Modeling and Control Strategy of Wind Energy Conversion System with Grid-Connected Doubly-Fed Induction Generator," *Energies*, vol. 15, no. 18, p. 6694, 2022, https://doi.org/10.3390/en15186694.

[41] N. A. N. Aldin, W. S. E. Abdellatif, Z. M. S. Elbarbary, A. I. Omar and M. M. Mahmoud, "Robust Speed Controller for PMSG Wind System Based on Harris Hawks Optimization via Wind Speed Estimation: A Real Case Study," *IEEE Access*, vol. 11, pp. 5929-5943, 2023,

https://doi.org/10.1109/ACCESS.2023.3234996.

[42] M. M. Mahmoud, M. K. Ratib, M. M. Aly, A. Moamen, and M. A. Rahim, "Effect of Grid Faults on Dominant Wind Generators for Electric Power System Integration : A Comparison and Assessment," *Energy Systems Research*, vol. 4, no. 3, pp. 70-78, 2021, https://doi.org/10.38028/esr.2021.03.0007.

[43] B. Yang, L. Jiang, L. Wang, W. Yao, and Q. H. Wu, "Nonlinear maximum power point tracking control and modal analysis of DFIG based wind turbine," *International Journal of Electrical Power & Energy Systems*, vol. 74, pp. 429-436, 2016, https://doi.org/10.1016/j.ijepes.2015.07.036.

[44] S. Gupta and A. Shukla, "Improved dynamic modelling of DFIG driven wind turbine with algorithm for optimal sharing of reactive power between converters," *Sustainable Energy Technologies and Assessments*, vol. 51, p. 101961, 2022, https://doi.org/10.1016/j.seta.2022.101961.

[45] M. M. Mahmoud *et al.*, "Integration of Wind Systems with SVC and STATCOM during Various Events to Achieve FRT Capability and Voltage Stability: Towards the Reliability of Modern Power Systems," *International Journal of Energy Research*, vol. 2023, no. 1, pp. 1-28, 2023, https://doi.org/10.1155/2023/8738460.

[46] B. S. Atia *et al.*, "Applications of Kepler Algorithm-Based Controller for DC Chopper: Towards Stabilizing Wind Driven PMSGs under Nonstandard Voltages," *Sustainability*, vol. 16, no. 7, p. 2952, 2024, https://doi.org/10.3390/su16072952.

[47] F. E. V. Taveiros, L. S. Barros, and F. B. Costa, "Back-to-back converter state-feedback control of DFIG (doubly-fed induction generator)-based wind turbines," *Energy*, vol. 89, pp. 896-906, 2015, https://doi.org/10.1016/j.energy.2015.06.027.

[48] A. A. Ansari, G. Dyanamina and A. A. Ansari, "Decoupled Control of Rotor Side Power Electronic Converter for Grid Connected DFIG Based Wind Energy System," *2023 IEEE International Students' Conference on Electrical, Electronics and Computer Science (SCEECS)*, pp. 1-6, 2023, https://doi.org/10.1109/SCEECS57921.2023.10063093.

[49] M. Soomro *et al.*, "Performance Improvement of Grid-Integrated Doubly Fed Induction Generator under Asymmetrical and Symmetrical Faults," *Energies*, vol. 16, no. 8, p. 3350, 2023, https://doi.org/10.3390/en16083350.

[50] K. Sabzevari *et al.*, "Low-voltage ride-through capability in a DFIG using FO-PID and RCO techniques under symmetrical and asymmetrical faults," *Scientific Reports*, vol. 13, 2023, https://doi.org/10.1038/s41598-023-44332-y.

[51] R. Sitharthan, C. K. Sundarabalan, K. R. Devabalaji, S. K. Nataraj, and M. Karthikeyan, "Improved fault ride through capability of DFIG-wind turbines using customized dynamic voltage restorer," *Sustainable Cities and Society*, vol. 39, pp. 114-125, 2018, https://doi.org/10.1016/j.scs.2018.02.008.

[52] S. R. K. Joga *et al.*, "Applications of tunable-Q factor wavelet transform and AdaBoost classier for identification of high impedance faults: Towards the reliability of electrical distribution systems," *Energy Exploration & Exploitation*, 2024, https://doi.org/10.1177/01445987241260949.